

DOUBLE-SQUARE ROOT TRAVELTIME APPROXIMATION FOR CONVERTED WAVES

I. Abakumov, B. Schwarz, C. Vanelle, B. Kashtan, and D. Gajewski

email: *abakumov_ivan@mail.ru*

keywords: *Time imaging, moveout, converted waves*

ABSTRACT

Over the past years, multi-parameter stacking has become a standard tool for seismic reflection data processing. Although several traveltimes approximations for converted waves may be found in the literature, all of them are designed for CMP-based observation geometry. In this paper we propose a double-square root traveltimes approximation for converted waves from a curved interface. This approximation is appropriate for large offsets. In the special case of monotypic waves it gives comparable results with other multi-parameter moveout formulas. Furthermore, we demonstrate that a CRS-type traveltimes approximation for converted waves may be derived from the new approximation. In this context, we also discuss a pragmatic search strategy. The key step of the strategy is the simulation of a zero-offset section by a stack of γ -CMP gathers, which may be considered as a first approximation of common conversion point gathers. For non-converted waves this approach transforms to the well-known pragmatic approach by Müller et al. (1998). The new operator does not require separation of PP and PS wavefields prior to stacking. In our examples, the effective wavefield attributes of converted and monotypic waves obtained by the corresponding type of the operator have comparable values and may be used in joint interpretation.

INTRODUCTION

Time imaging is less sensitive to velocity errors than depth imaging. For this reason, it is often carried out as a first imaging step, especially for the interpretation of complex models (Landa, 2008). It represents a convenient and efficient way to obtain a simulated zero-offset section from multi-coverage seismic data by summing along stacking surfaces in CMP data, and to extract wavefield parameters (attributes) in order to use them in subsequent imaging steps. Stacking significantly reduces the amount of data and increases the signal-to-noise ratio (Sengbush, 1983). To stack reflection and diffraction events it is necessary to have a traveltimes moveout expression for a family of source-receiver pairs in a distribution suitable to map the chosen imaging point. The quality of the ZO section and wavefield parameters significantly depends on the chosen stacking operator.

Of the existing techniques the following two are known to produce acceptable results for monotypic waves: multifocusing (MF Gelchinsky et al., 1999a,b) and the Common-Reflection-Surface stack (CRS) (Müller et al., 1998; Jäger et al., 2001). Stacking operators expressed by these techniques take into account the curvature of the reflection interface. In the 2D case they are parameterized by three fundamental wavefront attributes: the emergence angle β and the radii of the normal and normal-incidence point waves, R_N and R_{NIP} , respectively (Hubral, 1983). The MF/CRS stack is determined by a measure of the coherency of the multi-coverage data for any possible combination of attributes. This search of the global maximum of the coherency measure in the three-parametric attribute domain turns out to be a time-consuming problem. To relax the computational demand the so-called pragmatic approach was introduced. The CRS pragmatic

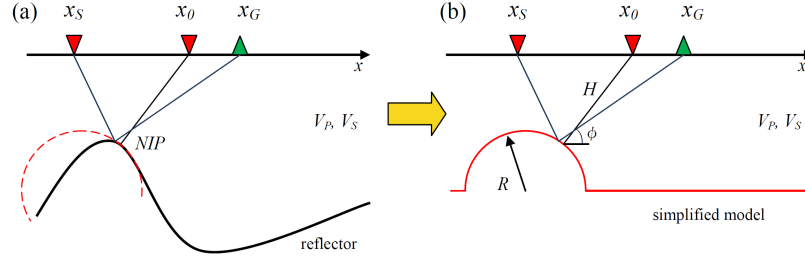


Figure 1: One-layer model with curved reflector. a) Principal scheme. b) Simplified model. Geometrical meaning of parameters R , H and ϕ .

approach (Müller, 1998) allows to split the simultaneous three-parameter search problem into three one-parametric searches and an optional final three-parametric local optimization. The CRS method gained significant advantages in terms of computing time by this strategy.

It is a more difficult problem to find powerful coherency-based stacking technique to enhance converted (e.g., PS or SP) reflections in pre-stack seismic data than to stack non-converted (PP or SS) reflections (Bergler et al., 2002). Approaches for stacking converted waves as, for instance, by common-midpoint (CMP) or common-conversion point stack were proposed by Tessmer and Behle (1988), Tessmer et al. (1990) and Iverson et al. (1989).

The aim of this study was to obtain traveltime approximations of converted waves valid for arbitrary observation geometry and arbitrary reflector curvature. In this paper, we propose a new traveltime approximation for converted waves and a pragmatic search strategy, which is based on the CRS approach and accounts for the asymmetry of PS trajectories. Finally, we present numerical simulations that provide insight into the accuracy of the new approximation in comparison with the exact solution. Effective attributes of converted and non-converted waves obtained by the corresponding type of operator tend to be comparable and may be used in further interpretation.

DOUBLE SQUARE ROOT TRAVELTIME APPROXIMATION FOR CONVERTED WAVES

Consider a central point x_0 , a source point x_S and a receiver point x_G at the surface $z = 0$ above a 2-D constant-velocity medium and a curved reflector of arbitrary shape (Figure 1a). The reflection traveltime for a converted PS wave as a function of the reflection point (x_{ref}, z_{ref}) is:

$$t_{PS} = \frac{1}{V_P} \sqrt{(x_S - x_{ref})^2 + z_{ref}^2} + \frac{1}{V_S} \sqrt{(x_G - x_{ref})^2 + z_{ref}^2}. \quad (1)$$

If all source-receiver pairs are located in the vicinity of central point x_0 , then all reflection points are located in the close vicinity of the normal-incidence-point (NIP) and hence the reflector may be accurately approximated by a circle (Figure 1b).

It is assumed that three additional parameters are known: the distance from the central point to the reflector H , the emergence angle ϕ , and the radius of curvature of the reflector R at the NIP. Approximating the interface by the circle with radius R and assuming that the distance from the central point to the source Δx_S or the receiver Δx_G is much smaller than the characteristic distance of problem (such as R or H) we obtain the following expression for the reflection point coordinates:

$$\begin{pmatrix} x_{ref} \\ z_{ref} \end{pmatrix} = \begin{pmatrix} \sin \phi & \cos \phi \\ -\cos \phi & \sin \phi \end{pmatrix} \begin{pmatrix} R \sin \alpha \\ R \cos \alpha - (R + H) \end{pmatrix},$$

where the angle α describes the deviation between the reflection point and the NIP. In Appendix A we

show that

$$\sin \alpha = \frac{\gamma \Delta x_G + \Delta x_S}{(1 + \gamma)(R + H)} \sin \phi + O(\varepsilon^2), \quad \varepsilon = \max\left(\frac{\Delta x_S}{R_N}, \frac{\Delta x_G}{R_N}, \frac{\Delta x_S}{R_{\text{NIP}}}, \frac{\Delta x_G}{R_{\text{NIP}}}\right), \quad \varepsilon \ll 1. \quad (2)$$

where γ is the ratio of velocities of the P- and S-waves and ε is a small parameter.

Substituting the reflection point approximation into equation (1), after a number of algebraic simplifications, we obtain the traveltine approximation t^{Sq} :

$$t^{Sq} = \frac{t_0}{1 + \gamma} \sqrt{1 + \frac{2\Delta x_S \sin \beta}{R_{\text{NIP}}} + \frac{\Delta x_S^2}{R_{\text{NIP}}^2} + \left(\frac{\gamma \Delta x_G + \Delta x_S}{1 + \gamma} - 2x_S\right) \frac{\gamma \Delta x_G + \Delta x_S \cos^2 \beta}{1 + \gamma} \frac{1 - \frac{R_{\text{NIP}}}{R_N}}{R_{\text{NIP}}^2}} + \frac{\gamma t_0}{1 + \gamma} \sqrt{1 + \frac{2\Delta x_G \sin \beta}{R_{\text{NIP}}} + \frac{\Delta x_G^2}{R_{\text{NIP}}^2} + \left(\frac{\gamma \Delta x_G + \Delta x_S}{1 + \gamma} - 2x_G\right) \frac{\gamma \Delta x_G + \Delta x_S \cos^2 \beta}{1 + \gamma} \frac{1 - \frac{R_{\text{NIP}}}{R_N}}{R_{\text{NIP}}^2}}. \quad (3)$$

For the purpose of convenience we use CRS parameters in (2) and (3), i.e., a variable change from (R, H, ϕ) to $(R_N, R_{\text{NIP}}, \beta)$ was made. The connection between the parameters is given by

$$R = R_N - R_{\text{NIP}}, \quad H = R_{\text{NIP}}, \quad \phi = \frac{\pi}{2} - \beta.$$

The approximation t^{Sq} is valid for any general location of the source and receiver points x_S and x_G . It can also be applied in other acquisition geometries than surface seismic, e.g., in vertical seismic profiling geometry. If we let the radius of curvature R go to infinity, we obtain the formula for the traveltine of a wave reflected from a planar interface. Setting $R = 0$ leads to the exact solution for diffracted waves (Landa et al., 2010). In the case $\gamma = 1$ we obtain multi-parameter moveout corrections like MF or CRS. Although the t^{Sq} approximation was derived for the constant velocity overburden, it is applicable for any arbitrary velocity model. In that case, the wavefield attributes $(R_N, R_{\text{NIP}}, \beta)$ lose their clear geometrical interpretation and become effective parameters.

PRAGMATIC SEARCH STRATEGY FOR CONVERTED WAVES

The stacking procedure consists of evaluating a measure of the coherency of the multi-coverage data along traveltine surfaces given by the t^{Sq} approximation (3) for any possible combination of wavefield parameters. The determination of the global maximum of the coherency turns out to be too time consuming in a three-parametric search strategy. Therefore, we propose a pragmatic search strategy, that helps to split the three-parametric search problem into four one-parametric searches and an optional three-parametric local optimization.

The CRS stack approach determines optimal values of wavefield attributes for a known near-surface velocity. For converted waves we additionally require that the near-surface velocities ratio γ is known. The first search step of the CRS pragmatic approach is an automatic common midpoint (CMP) stack. However, since the path of the converted wave is asymmetrical, successful stacking of converted waves can not be achieved using common midpoint gathers, but requires a common conversion point (CCP) gather (Tessmer and Behle, 1990). For complex models the conversion point can be established only by iterative methods, e.g. ray tracing, which requires P- and S-velocity models.

For a single horizontal homogeneous layer, Fromm et al. (1985) derived the relation $x_p = \gamma x / (1 + \gamma)$ with $\gamma = V_P / V_S$ as a first-order approximation for the horizontal distance x_p of the conversion point from the source point. Following this idea, we propose to construct γ -CMP gathers: we introduce γ -CMP coordinates \tilde{x}_m and \tilde{h} . These coincide with the standard CMP coordinates in the particular case of monotypic waves. γ -CMP gathers may be considered as the first linear approximation of CCP gathers. Furthermore, we define the inverse of an effective velocity V_{eff} as the algebraic average of the inverse P- and S-wave velocities. In summary, we use

$$\frac{2}{V_{eff}} = \frac{1}{V_P} + \frac{1}{V_S}; \quad t_0 = \frac{2R_{\text{NIP}}}{V_{eff}}; \quad \tilde{x}_m = \frac{x_S + \gamma x_G}{1 + \gamma}; \quad \tilde{h} = \frac{x_G - x_S}{1 + \gamma}; \quad \Delta \tilde{x}_m = \tilde{x}_m - x_0.$$

The variable change from the source-receiver (x_S, x_G) domain to the (\tilde{x}_m, \tilde{h}) domain and the Taylor expansion of the square roots in the t^{Sq} approximation (3) omitting all terms of order higher than two leads us to the CRS-type formula for converted waves in γ -CMP coordinates:

$$t_{\gamma\text{-CRS}}^2 = \left(t_0 + \frac{2 \sin \beta}{V_{eff}} \Delta \tilde{x}_m \right)^2 + \frac{2 t_0 \cos^2 \beta}{V_{eff}} \left(\frac{\Delta \tilde{x}_m^2}{R_N} + \frac{\gamma \tilde{h}^2}{R_{NIP}} \right). \quad (4)$$

This formula illustrates the close relation between the t^{Sq} approximation and the CRS pragmatic approach. In case of monotypic waves (i.e., $\gamma = 1$) it coincides with the CRS stacking operator.

If standard CMP coordinates are substituted in (4) we obtain the same five parameter expression that was derived by Vanelle et al. (2011). It is formally identical with that of Bergler et al. (2002).

Using Equation (4) we can now formulate a pragmatic approach for converted waves similar to the one suggested by Müller et al. (1998). It consists of the following steps:

1. Automatic γ -CMP search with $\Delta \tilde{x}_m = 0$:

$$t_{\gamma\text{-CMP}}^2 = t_0^2 + \frac{2 t_0 \gamma \tilde{h}^2 q}{V_{eff}}; \quad q = \frac{\cos^2 \beta}{R_{NIP}}.$$

Output: ZO section, combined parameter q .

2. Plane wave search in the ZO section with $\tilde{h} = 0$:

$$t_{\gamma\text{-PW}} = t_0 + \frac{2 \sin \beta}{V_{eff}} \Delta \tilde{x}_m.$$

Output: emergence angle β .

3. Repeated γ -CMP search with $\Delta \tilde{x}_m = 0$. Fromm et al. (1985) showed that the traveltime of converted waves expanded into a power series comprise terms of third order that depend on the emergence angle and R_{NIP} . Due to this fact, the determination of R_{NIP} from the combined parameter q and angle β is not an accurate procedure. For these reasons an additional R_{NIP} search is required:

$$t^{Sq} = \frac{R_{NIP}}{V_P} \sqrt{1 - \frac{2 \gamma \tilde{h} \sin \beta}{R_{NIP}} + \frac{\gamma^2 \tilde{h}^2}{R_{NIP}^2}} + \frac{R_{NIP}}{V_S} \sqrt{1 + \frac{2 \tilde{h} \sin \beta}{R_{NIP}} + \frac{\tilde{h}^2}{R_{NIP}^2}} - \left(t_0 - \frac{2 R_{NIP}}{V_{eff}} \right).$$

Output: radius of NIP wave.

4. Hyperbolic search in the ZO section with $\tilde{h} = 0$:

$$t_{\gamma\text{-HY}}^2 = \left(t_0 + \frac{2 \sin \beta}{V_{eff}} \Delta \tilde{x}_m \right)^2 + \frac{2 t_0 \Delta \tilde{x}_m^2 \cos^2 \beta}{V_{eff} R_N}.$$

Output: radius of normal wave R_N .

After the determination of the wavefield attributes (β, R_{NIP}, R_N) the local optimization is carried out with the t^{Sq} stacking operator (3). The final ZO section from the multi-coverage data is then constructed for the attributes of this optimization.

NUMERICAL EXAMPLES

In this section we provide insight into the accuracy and the range of applicability of the t^{Sq} approximation with examples. We begin with simple models like a constant velocity and constant vertical gradient overburden over a circular reflector to demonstrate the accuracy of the traveltime approximation and the coefficient determination. Using a more complex synthetic data set we show that the new formulation also

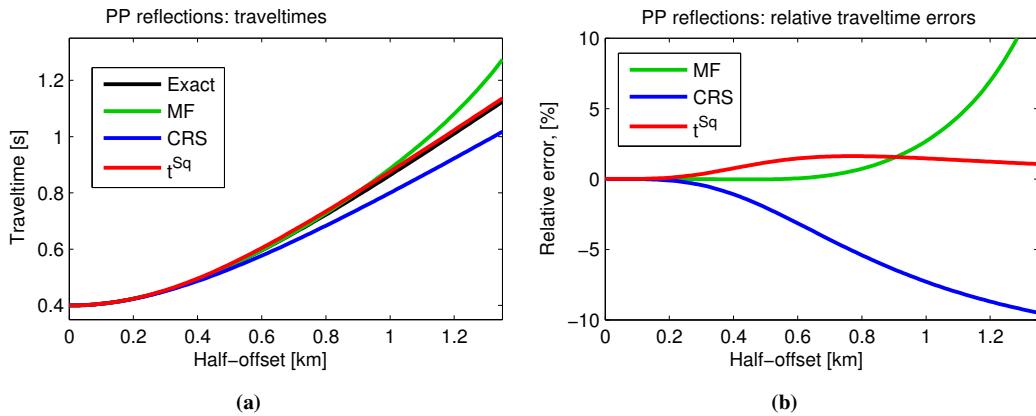


Figure 2: Accuracy of traveltime approximations for monotypic waves. (a) Comparison of the reference traveltime (black), MF (green), CRS (blue) and t^{Sq} (red) approximations. (b) Relative errors of the MF (green), CRS (blue), and t^{Sq} (red) approximations.

leads to high quality stack results.

Let us consider the velocity model from Figure 1b with a circular reflector under a homogeneous overburden. For monotypic reflections, the reflection point can be found by evaluating the roots of a fourth-order equation (e.g., Drexler and Gander, 1998). For converted waves the exact solution requires solving a sixth-order polynomial, which can be achieved with high accuracy by numerical methods (e.g., Abakumov and Kashtan, 2011). We calculated such solutions as reference traveltimes. For the accuracy studies we used a model with $R_{NIP} = 0.5$ km, $R_N = 1.0$ km, $\beta = 30^\circ$, and the near-surface velocities $V_P = 2.5$ km/s and $V_S = 1.8$ km/s.

For monotypic waves the accuracy of the t^{Sq} approximation can be compared not only with the reference traveltime, but as well with the CRS and MF approximations. The resulting t^{Sq} , CRS, MF approximations and the reference traveltimes in a (standard) CMP gather with a maximum offset of 1.35 km are presented in Figure 2a. These are compared to the reference traveltimes in Figure 2b where relative errors are shown. We observe that the t^{Sq} approximation exhibits smaller errors for large offsets than MF and CRS, although MF is more accurate for small offsets.

There is no converted wave expression for the MF approximation or CRS. For these reasons, for con-

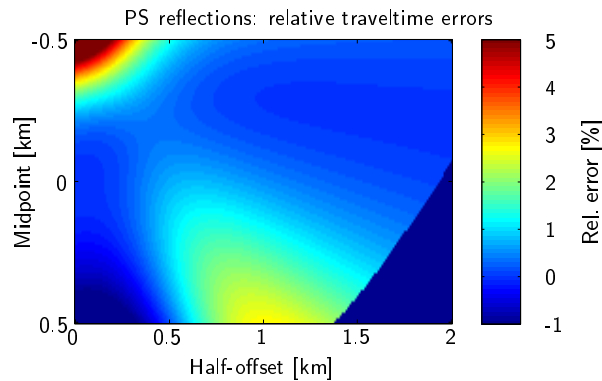


Figure 3: Relative traveltime errors of the t^{Sq} approximation for converted waves.

verted waves the t^{Sq} approximation was only compared to the exact solution. The resulting relative errors are shown in Figure 3. We find that in most regions the error is less than 2%.

In order to investigate the accuracy of the coefficients, we have chosen a medium with a constant vertical velocity gradient, $V_P = 2.0 + 1.0z$ km/s and $\gamma = 1.4$ with a circular reflector with the radius $R = 1.0$ km and its midpoint at a depth $H = 2.0$ km. Reference solutions for the wavefield attributes were generated by a numerical determination of the reflection and conversion points and subsequent evaluation of results given in Vanelle (2002). A total of 201 cdp points were used for the stack with a spacing of 0.025 km, and offsets varying from 0.0 to 2.0 km. Noise with $S/N = 5.0$ was added to all traces.

Figure 4 illustrates the semblance, emergence angle, R_{NIP} , K_N for PP as well as PS reflections, and in comparison to the reference values. The wavefield attributes are now effective parameters, which do not have a clear geometrical interpretation any more.

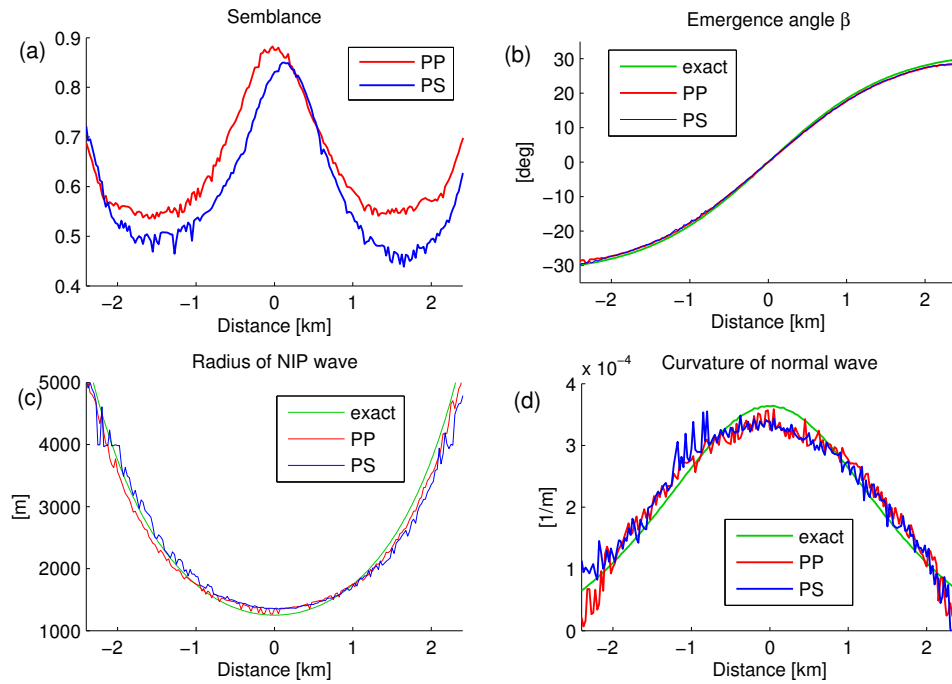


Figure 4: Semblance (a) and effective wavefield attributes (b)-(d), derived from converted (blue) and monotypic (red) waves by applying the t^{Sq} operator. The effective wavefield attributes tend to have similar behavior in comparison to the exact values (yellow). The asymmetry in the semblance (a) may be explained by the asymmetry of the survey.

Finally, we have applied the new operator to a complex synthetic dataset. The NORSAR ray tracing package was used to generate synthetic seismograms for the model shown in Figure 5. The resulting PP- and PS-stacked sections in Figure 6 exhibit similar quality. Due to the asymmetry of the PS ray paths, we observe a better illumination of the distant part of the top reflector in the PS than in the PP stack. We conclude that joint interpretation of PP- and PS-stacked data using the t^{Sq} operator allows for a better understanding of the subsurface structure.

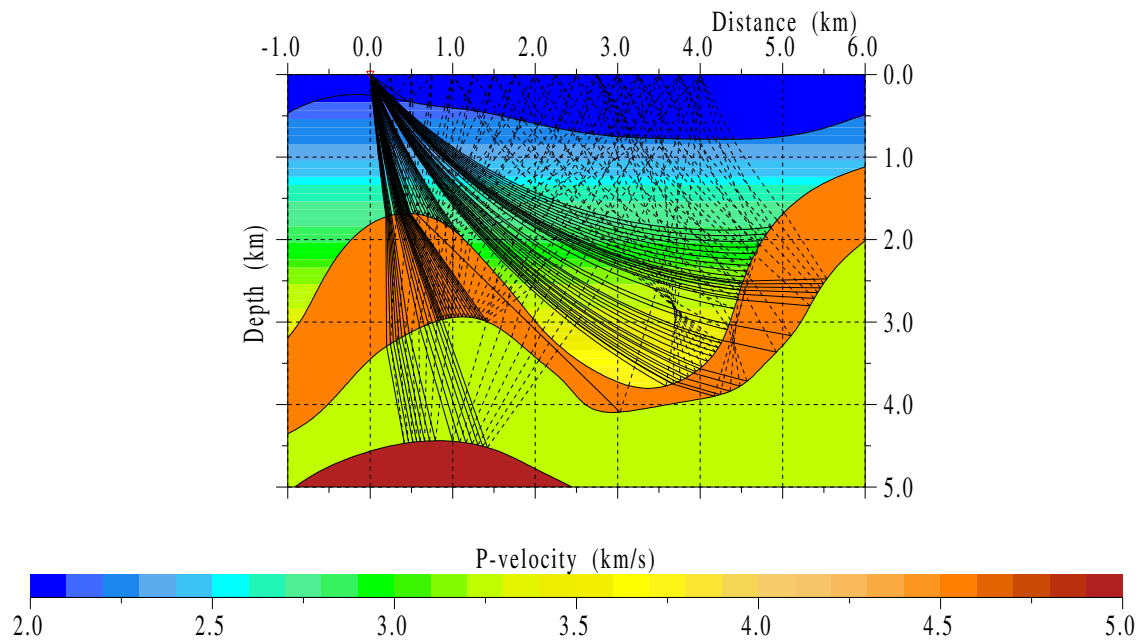


Figure 5: Complex velocity model consisting of a homogeneous low velocity near-surface layer, a gradient second layer and three underlying constant velocity layers. The V_P/V_S ratio is $\gamma = 1.73$ in the near-surface layer and $\gamma = 1.80$ in the remaining model parts.

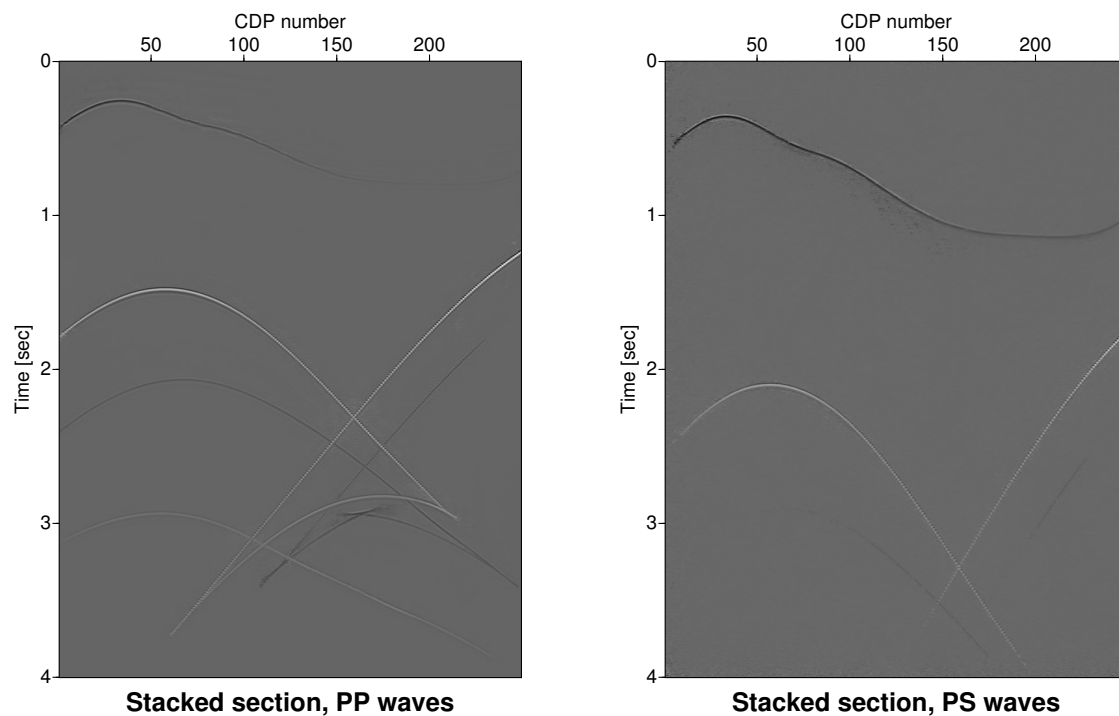


Figure 6: Stacked section for PP and PS waves. Note the continuity of the top reflector in the PS section resulting from the asymmetric ray paths.

CONCLUSIONS

We have introduced a new non-hyperbolic traveltime expression, the t^{Sq} approximation, for converted wave reflections from curved interfaces. For monotypic waves and large offsets, the new formulation leads to higher accuracy than multifocusing (MF) and CRS. For converted waves, where equivalent expressions to MF or CRS are not available, the new operator is also highly accurate.

Further more, we have derived a CRS-type expression for converted waves from the t^{Sq} approximation. This hyperbolic operator is expressed in γ -CMP coordinates and allows for a pragmatic search strategy also for the t^{Sq} operator for converted waves. The key step of the strategy is the simulation of the ZO section by the stack of γ -CMP gathers, which may be considered as the first approximation of CCP gathers. For the case of monotypic waves this approach reduces to the well-known pragmatic CRS search strategy of Müller (1998).

Effective attributes of converted and monotypic waves obtained by the corresponding type of t^{Sq} operator provide comparable PP and PS images and may be used in a joint interpretation. The asymmetrical ray paths of converted waves allow to generate better images of inclined parts of the reflector since monotypic and converted waves image different parts of the reflector.

ACKNOWLEDGMENTS

This work was kindly supported by the sponsors of the Wave Inversion Technology Consortium and by State Contract RF N 02.740.11.0331. Special thanks to NORSAR Innovation AS for allowing us to use their seismic modeling software.

REFERENCES

- Abakumov, I. V. and Kashtan, B. M. (2011). Traveltime approximation for converted waves. *73rd EAGE Conference & Exhibition*, P072.
- Bergler, S., Duveneck, E., Höcht, G., Zhang, Y., and Hubral, P. (2002). Common-reflection-surface stack for converted waves. *Studia Geophysica et Geodaetica*, 46(2):165–175.
- Drexler, M. and Gander, M. (1998). Circular billiard. *SIAM Review*, 40:315–323.
- Fromm, G., Krey, T., and Wiest, B. (1985). *Seismic Shear Waves. Chapter: Static and dynamic corrections*. Geophysical Press, Handbook of Geophysical Exploration, Vol. 15a. 191-225.
- Gelchinsky, B., Berkovitch, A., and Keydar, S. (1999a). Multifocusing homeomorphic imaging, part 1. basis concepts and formulas. *Journal of Applied Geophysics*, 42:229–242.
- Gelchinsky, B., Berkovitch, A., and Keydar, S. (1999b). Multifocusing homeomorphic imaging, part 2. multifold data set and multifocusing. *Journal of Applied Geophysics*, 42:243–260.
- Hubral, P. (1983). Computing true amplitude reflections in a laterally inhomogeneous earth. *Geophysics*, 48:1051–1062.
- Iverson, W. P., Fahmy, B. A., and Smithson, S. B. (1989). v_p/v_s from mode-converted p-sv reflections. *Geophysics*, 54:843–852.
- Jäger, R., Mann, J., Höcht, G., and Hubral, P. (2001). Common reflection surface stacking stack: Image and attributes. *Geophysics*, 66.
- Landa, E. (2008). *Beyond Conventional Seismic Imaging*. EAGE.
- Landa, E., Keydar, S., and Moser, T. J. (2010). Multifocusing revisited - inhomogeneous media and curved interfaces. *Geophysical Prospecting*, 57.
- Müller, T. (1998). Common reflection surface stack versus nmo/stack and nmo/dmo/stack. *60th Mtg. Eur. Assoc. Expl. Geophys.*

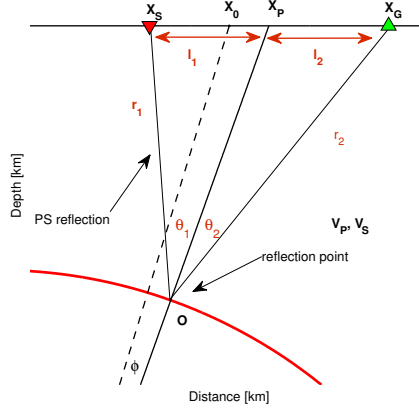


Figure 7: Reflection on a circular reflector (red) with mid-point R : basic notations.

Müller, T., Jäger, R., and Höcht, G. (1998). Common reflection surface stacking method - imaging with a unknown velocity model. *68th Ann. Internat. SEG Mtg., New Orleans, USA, Expanded Abstracts*, 57:1764–1767.

Sengbush, R. (1983). *Seismic Exploration Methods. Chapter 4: Analysis and Suppression of Seismic Noise*. IHRDC, Boston. pp. 43-88.

Tessmer, G. and Behle, A. (1988). Common reflection point data-stacking technique for converted waves. *Geophysical Prospecting*, 36:671–688.

Tessmer, G. and Behle, A. (1990). *Velocity Analysis on Multichannel Seismic Data. Chapter: Common reflection point data-stacking technique for converted waves*. SEG, Tulsa. 328-345.

Tessmer, G., Krajewski, P., Fertig, J., and Behle, A. (1990). Processing of ps-reflection data applying a common conversion-point stacking technique. *Geophysical Prospecting*, 38:267–286.

Vanelle, C. (2002). *Traveltime-based true-amplitude migration*. PhD thesis, University of Hamburg.

Vanelle, C., Kashtan, B., Dell, S., and Gajewski, D. (2011). A CRS-type stacking operator for converted waves. *15th Annual WIT report*.

APPENDIX A

In this appendix, we derive equation (2) for $\sin \alpha$. Let us consider a circular reflector with its center denoted by R , a central point X_0 , and a source and receiver at X_S , X_G , respectively (see Figure 7). Then we can express the deviation angle $\alpha = \angle X_0 R X_P$ between the reflection point and the normal incidence point by the relations in the triangle:

$$\sin \alpha = \frac{X_0 X_P}{R X_P} \sin(\pi - \phi) = \frac{X_0 X_P}{R X_P} \sin \phi = \frac{X_0 X_P}{X_0 R} \sin \phi (1 + O(\epsilon)). \quad (5)$$

The combination of the Snell's Law and the relations in the triangles $X_S O X_P$, $X_G O X_P$,

$$\frac{\sin \theta_1}{V_p} = \frac{\sin \theta_2}{V_s}, \quad \frac{l_1}{\sin \theta_1} = \frac{r_1}{\sin \beta}, \quad \frac{l_2}{\sin \theta_2} = \frac{r_2}{\sin(\pi - \beta)},$$

lead to the following estimation of the ratio l_1/l_2 :

$$\frac{l_1}{l_2} = \frac{V_p r_1}{V_s r_2} = \gamma \frac{r_1}{r_2} = \gamma(1 + O(\epsilon)). \quad (6)$$

Here we took into account that $\varepsilon \ll 1$ from (2), hence $H \gg l_1, H \gg l_2$ and

$$\frac{r_1}{r_2} = \frac{\sqrt{H^2 - 2Hl_1 \cos \phi + l_1^2}}{\sqrt{H^2 + 2Hl_2 \cos \phi + l_2^2}} = 1 + O(\varepsilon).$$

Combination of (6) and the fact that $l_1 + l_2 = X_G - X_S$ yields the following expression for $X_0 X_P$:

$$X_0 X_P = \frac{\gamma \Delta x_G + \Delta x_S}{1 + \gamma} (1 + O(\varepsilon)),$$

where a variable change from X_S, X_G to $\Delta x_S = X_S - X_0, \Delta x_G = X_G - X_0$ was made. Substituting $X_0 X_P$ into equation (5) gives the final result

$$\sin \alpha = \frac{\gamma \Delta x_G + \Delta x_S}{(1 + \gamma) R_N} \sin \phi + O(\varepsilon^2).$$